2.6 Foregrounds (4 pgs, Jacques and Clem)

The state of knowledge and known challenges; how does PICO address the challenges; forecast of performance.

2.7 Systematic Errors (3 pgs, Crill)

In developing the theoretical framework for measuring the faint CMB polarization signal, the CMB community has long recognized the impacts of systematic errors due to instrumentation and data analysis. A rich literature investigates the types of systematic errors that confound the polarization measurement and ways to mitigate them[1]. Each on-orbit measurement of CMB polarization was limited by sysetmatic errors until an in-depth study of the systematics was performed and the post-processing data analysis removed them as well as possible[2, 3]. Additionally, recently proposed CMB missions, such as LiteBird and CORE, have placed systematic error mitigation at the forefront of the case for their mission[4, 5, 6].

Note: Calculate a defensible level of acceptable systematics. For example, integrate r 10^{-3} and 10^{-4} power from ell 2-10, 10-50,(do a signal to noise calculation), then state what map rms that corresponds to.

A CMB mission aiming for the unprescedented sensitivity of PICO must control systematic errors to avoid bias or an increased variance of the science measurement. Systematics must be controlled or corrected to a level that enables the PICO science goals (better than 1 nanoKelvin (**Note: make sure this is a correct statement - also be careful about reducing a complicated concept such as systematic errors to a single map rms number, could also quote this as a δr error**) in the map). Mitigation of systematic errors is the most important reason (along with the availability of broad wavelength coverage) to perform a measurement of the CMB polarization from a space telescope; Compared with a ground-based, sub-orbital, or even a space mission in low-Earth orbit, the L2 environment offers excellent stability as well as the ability to observe large fractions of the sky on many time scales without interference from the Sun, Earth, or Moon. This redundancy of observations allows the checking of consisitency of results and an improved ability to correct systematic errors in post-processing analysis.

During the course of the PICO Study, a systematics working group examined systematic errors affecting PICO, Most systematic errors can be mitigated by careful design and engineering of the spacecraft and instrument, and the use of present-day state-of-the-art technology and data analysis tools. However, some systematic errors may limit the precision of the B-mode measurement and the group studied these in further detail. The work was based on the experience of the group's involvement with past missions, in particular Planck, and in recent detailed studies on the CORE and LiteBird concepts

End-to-end simulation of the experiment is an essential tool, including realistic instabilities and non-idealities of the spacecraft, telescope, instrument and folding in data post-processing techniques used to mitigate the effects. Systematics are coupled with the spacecraft scan strategy, and the details of the data analysis pipeline. During the study, the PICO team used simulation and analysis tools developed for the Planck mission[7] and the*CORE*mission concept, adapting them for PICO. These tools allowed a deeper examination of several key systematic errors.

2.7.1 List of Systematics

The systematic errors face by PICO can be categorized into three broad categories 1) Intensity-to-polarization leakage, 2) stability, and 3) straylight. These were prioritized for further study based on the team's assessment of how well these systematics are understood by the community, whether mitigation techniques exist - either in instrument design or in data analysis.

Name	Description	State-of-the-art	Additional Possible Mitigation
Leakage			
Bandpass Mismatch	Edges and shapes of the the spectral filters vary from detector to detector. leaks T $\rightarrow$ P, P $\rightarrow$ P leakage if the source's bandpass differs from calibrator's bandpass[**?**]	Precise bandpass measurement[**?**]; SRoll algorithm[**?**]; filtering technique[**?**];	polarization modulation; full I/Q/U maps for individual detectors mitigates; additional component solution (see Banerji& Delabrouille (in prep) **Current techniques may be adequate**
Beam mismatch		See Sect. 2.7.2	
Gain mismatch			
Time Response Accuracy and Stability			
Readout Cross-talk			
Polarization Angle			See Sect. 2.7.2
Cross-polarization			
Chromatic beam shape			
Stability			
Pointing jitter			
Gain Stability			See Sect. 2.7.3
Straylight			
Far Sidelobes			See Sect. 2.7.4
Other			
Residual correlated cosmic ray hits			

Table 1: Systematic errors expected to affect PICO.

2.7.2 Absolute polarization angle calibration

The rotation of the CMB polarization can have different causes, including 1. a birefringent primordial Universe, or a Faraday rotation due a primordial magnetic field [8], 2. birefringent foregrounds, or interaction with the Galactic magnetic field, 3. systematic effects in the instrument, and in particular an error on the actual direction of polarization measured by each detector. While the first two sources create a rotation that may depend on scale, position and/or frequency, the latter is expected to mostly depend on the detector considered.
A rotation α of the direction of polarization mixes the Q and U Stokes parameters via $Q \pm iU \longrightarrow e^{\mp i2\alpha}(Q \pm iU)$ and affects the power spectra via (assuming the rotation to be independent on scale and location)

$$C_\ell^{TT} \longrightarrow C_\ell^{TT} = C_\ell^{TT} \tag{1a}$$
$$C_\ell^{TE} \longrightarrow \cos 2\alpha\, C_\ell^{TE} \sim \left(1 - 2\alpha^2\right)\, C_\ell^{TE} \tag{1b}$$
$$C_\ell^{EE} \longrightarrow \cos^2 2\alpha\, C_\ell^{EE} + \sin^2 2\alpha\, C_\ell^{BB} \sim C_\ell^{EE} - 4\alpha^2\, \left(C_\ell^{EE} - C_\ell^{BB}\right) \tag{1c}$$
$$C_\ell^{BB} \longrightarrow \sin^2 2\alpha\, C_\ell^{EE} + \cos^2 2\alpha\, C_\ell^{BB} \sim C_\ell^{BB} + 4\alpha^2\, \left(C_\ell^{EE} - C_\ell^{BB}\right) \tag{1d}$$
$$C_\ell^{TB} \longrightarrow \sin 2\alpha\, C_\ell^{TE} \sim 2\alpha\, C_\ell^{TE} \tag{1e}$$
$$C_\ell^{EB} \longrightarrow \sin 2\alpha \cos 2\alpha \left(C_\ell^{EE} - C_\ell^{BB}\right) \sim 2\alpha\, \left(C_\ell^{EE} - C_\ell^{BB}\right) \tag{1f}$$

as illustrated in Fig. 1.

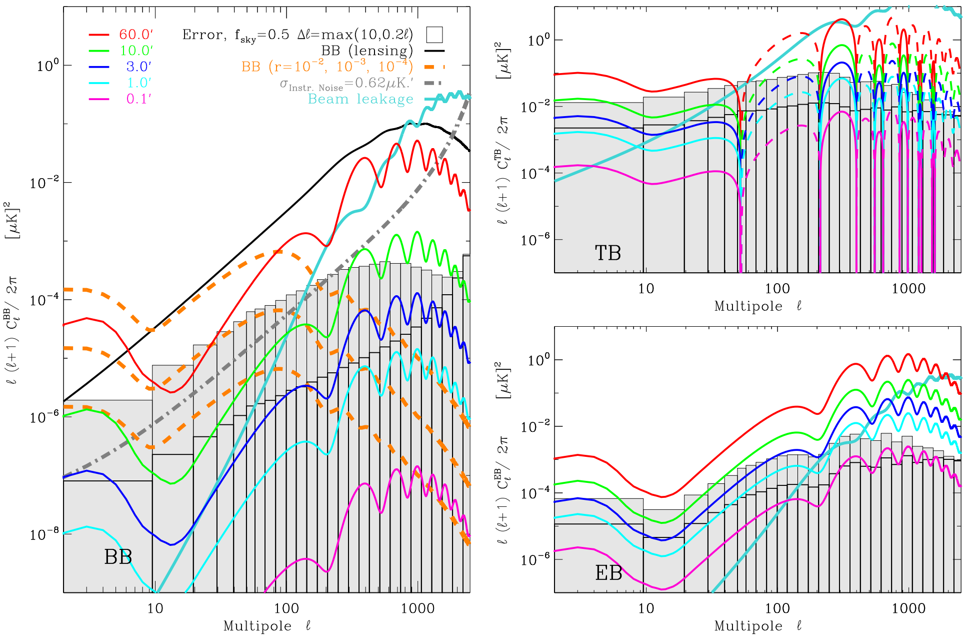

Figure 1: Effect of a rotation of the angle of polarization, assuming the Planck 2018 Λ-CDM best fit model [9] and expected PICOperformances, with a perfect delensing †[(the beam related systematics effects are still arbitrary; to be improved or removed)]†.

In Planck, the ground measurements of the detectors orientation had an error of $\pm 0.9^o$ (rel.) $\pm 0.3^o$ (abs.) [10].
The most recent constraints on cosmological birefringence (or systematic rotation) was set in **(author?)** [11], looking for residual signal in TB and EB spectra, but are dominated by the uncertainties on the detector orientations.
In PICO, the relative rotation of the detectors, could be measured with a good accuracy (a few $0.1'$?, †[refs?]†) on the CMB, but the overall rotation is difficult to determine. Known polarized sources, such as the Crab Nebula, could be used to do that but **(author?)** [12] show that the current uncertainty of $0.33^o = 20'$ on the Crab polarization orientation, obtained when combining all the available measurements, would not the measurement of tensorial B modes below $r \sim 0.01$ (assuming everything else to be nominal), far from PICO's target.
Figures 2 and 3 show how the measurement of r by PICO is degraded because of an overall rotation of polarization, and how TB and EB can be used to monitor precisely this rotation, assuming that the only source of polarization rotation is instrumental. These results are obtained assuming the spectra to have a Gaussian likelihood, with a variance $\propto 1/f_{\rm sky}$, and ignoring the foreground contributions.
TB and EB spectra can detect and measure a global polarisation rotation at levels ($0.1'$) well below those affecting r measurements in BB ($> 1'$). However, in doing such studies, one can not ignore other important aspects of the measurements of CMB polarization: For instance, one has to consider how the delensing will affect the B maps and their final noise levels. At large scales, the interaction with foregrounds makes masking necessary, which creates some extra E to B leakage, and complicates the estimation of B modes and of their likelihood. It also necessitates a proper component separation technique, especially in presence of finite and probably mismatched spectral bandwith of the detectors. The time correlation of the noise (with a $1/f$ spectral shape),

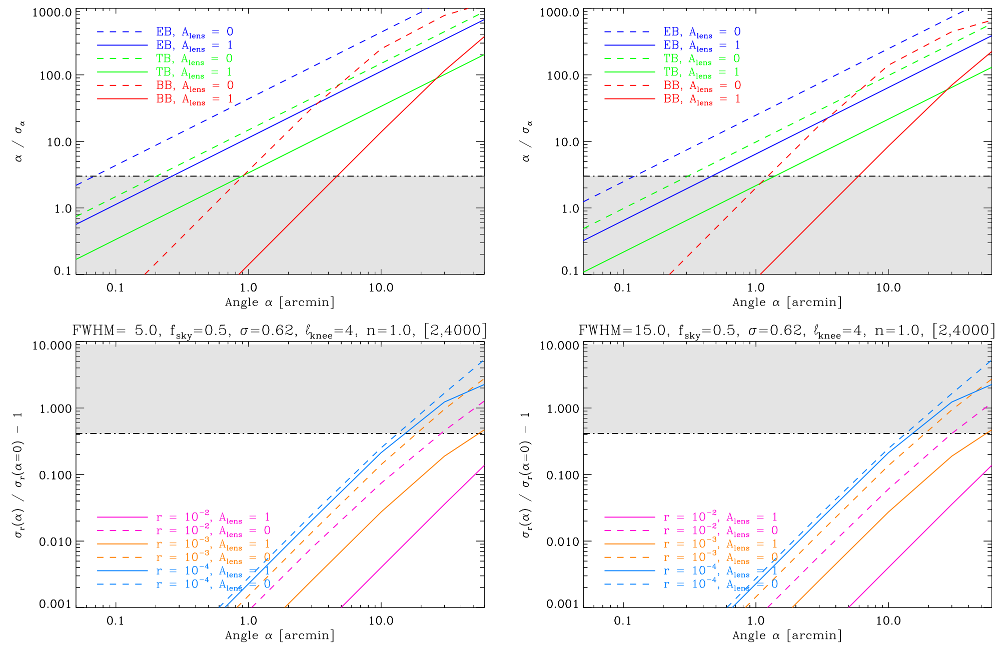

Figure 2: Upper panels: signal to noise ratio of the polarization angle α measurement by EB (blue lines), TB (green lines) and BB (red lines), assuming either no delensing (solid lines) or perfect delensing (dashes); the shaded area is $|\alpha|/\sigma_\alpha < 3$. Lower panels: degradation on measurement of r, for $r = 10^{-2}$, 10^{-3}, 10^{-4} (magenta, orange and cyan lines, respectively), either with no delensing (solid lines) or perfect delensing (dashes). The underlying cosmology is Planck 2018 Λ-CDM model (with $\tau = 0.054$), and assuming a polarized noise of rms = $0.62\mu K.'$ and power spectrum $(1 + (\ell_{\rm knee}/\ell)^n)$ with $\ell_{\rm knee} = 4$ and $n = 1$, with the analysis done on the multipole range $[2, 4000]$ over a sky fraction $f_{\rm sky} = 0.5$. The beam FWHM= $5'$ on the *lhs* and $15'$ on the *rhs* panels.

will also complicate the analysis. At intermediate and small scales, many other systematics, like those related to beams, will also have to be modeled.

2.7.3 Gain Stability

Photometric calibration is the process of converting the raw output of the receivers into a physically-meaningful quantity, such as thermodynamic temperature or brightness. As CMB receivers are usually linear, this process reduces to the characterization of the *gain factor* G:

$$y(t) = G(t) \times T\big(\vec{x}(t)\big) + n(t), \tag{2}$$

where $y(t)$ is the timestream of raw samples produced by the detector, $G(t)$ is the gain factor (which we allow to vary with time), T is the sky temperature observed along direction $\vec{x}(t)$ (which varies with time as the spacecraft spins), and $n(t)$ is a noise term that includes both uncorrelated and correlated noise. It is assumed that the timescale of variation in G ($G/\dot{G}$) is much longer than the typical timescale of variations in T: in the case of Planck, this was of the order of several days. In the case of space CMB experiments, the characterization of $G(t)$ is commonly done using the signal caused by the motion of the spacecraft with respect to the rest frame of the CMB itself. This signal is commonly called the *dipole*, as its most significant contribute is at multipole $\ell = 1$. For the PICO concept study, we evaluated the impact of noise in the estimation of $G(t)$ using the

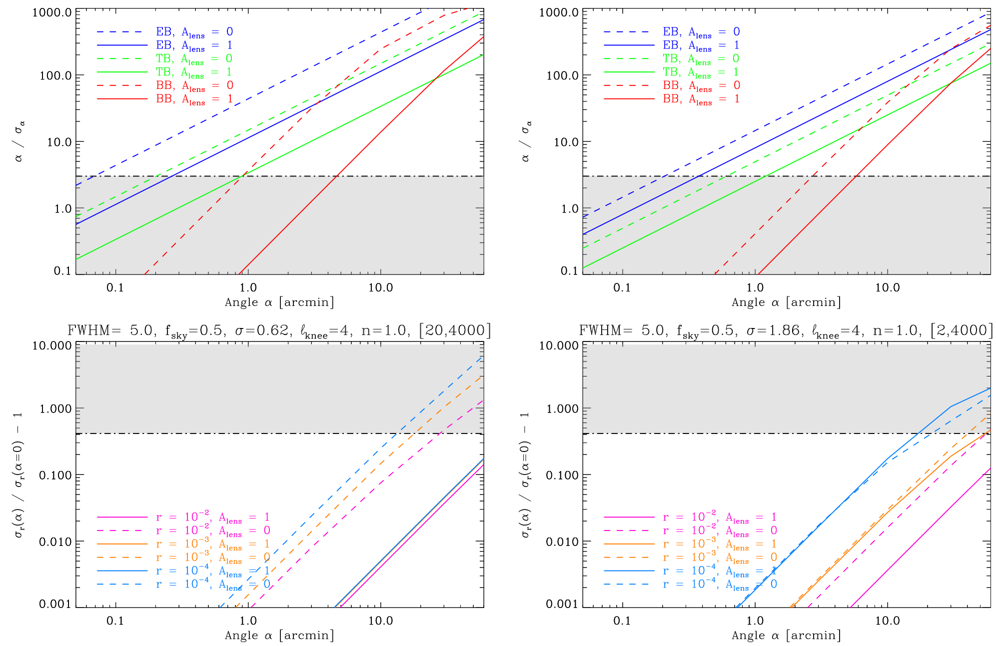

Figure 3: Same as Fig. 2, left panels, reducing the multipole range $[20, 4000]$ (*lhs*) or with a noise rms multiplied by 3 (*rhs*).

tools developed for the Planck/LFI instrument and the CORE mission proposal. The quality of the estimate depends on the noise level of the receiverse, but also on the details of the scanning strategy. The Planck/LFI experiment, because of a poor choice of the scanning strategy parameters (namely, a too slow precession motion), was forced to avoid using one year out of four in the 2015 data release [REF]. We can anticipate that this problem is not expected in PICO, thanks to the significantly faster precession envisaged.
In order to test the impact of calibration uncertainties, we have run the following analysis:

1. We simulated the observation of the sky, assuming four receivers and the nominal scanning strategy. We included both white noise and $1/f$ noise. The sky only contained CMB anisotropies, plus the CMB dipole.

2. We ran the calibration code to fit the dipole against the raw data simulated during step 1.

3. We simulated again the observation of the sky, but this time we used the values of G computed during step 2, which contain errors due to the presence of $n(t)$ and the CMB signal in Eq. (2). The noise in the output map is therefore the sum of the noise in the error on G and the term n.

The presence of foregrounds in the sky signal would cause a bias in the estimation of the calibration constants, due to the presence of large scale features in the Milky Way at microwave frequencies. A full data analysis pipeline for PICO should pair the calibration step with the component separation step, following a schema similar to what has been done by the Planck/LFI team for the 2018 data release [CITATION]: the application of the calibration code should be followed by a component separation analysis, and these two steps should be iterated until the result converge to a solution. In this analysis we assume to study the calibration at the last iteration, when the components have already been properly separated.

Results of the simulation are shown in Figures XXX and YYY. The scanning strategy employed by PICO allows for a much better calibration than in the case of Planck's, thanks to the much faster precession.

2.7.4 Far Sidelobe Pickup

...

2.7.5 Key Findings

Understanding and controlling the effects of systematic errors in a next-generation CMB probe is critical.
The raw sensitivity of the instrument should include enough margin that data subsets can independently archieve the science goals. This allows testing of the results in the data analysis and additional data cuts, if needed.
In a PICO mission's phase A, a complete end-to-end system-level simulation software facility would be developed to assist the team in setting requirements and conducting trades between subsystem requirements while realistically accounting for post-processing mitigation. Any future CMB mission is likely to have similar orbit and scan characteristics to those of PICO, thus there is an opportunity for NASA and the CMB community to invest in further development of this capability now.

3 Instrument (6 pgs, Hanany & Trangsrud)

Telescope (Hanany / Young), focal plane (Hanany / Young), cooling (Trangsrud), readout (O'Brient)
Review: Bock, Hubmayr, Suzuki,

4 Mission (5 pgs, Trangsrud)

To be included: mission architecture, spacecraft and subsystems, orbit, attitude control and determination (Trangsrud)

5 Technology Maturation (4 pgs, O'Brient & Trangsrud)

Requirements, planned activities, schedules and milestones, estimated cost (O'Brient?)
For each technology include:

- Requirements
- Planned activities
- Schedule and Milestones
- Estimated Cost

References

[1] W. Hu, M. M. Hedman, and M. Zaldarriaga. Benchmark parameters for CMB polarization experiments. *Phys. Rev. D.*, 67:043004–+, February 2003. astro-ph/0210096.

[2] C. L. Bennett, D. Larson, J. L. Weiland, N. Jarosik, G. Hinshaw, N. Odegard, K. M. Smith, R. S. Hill, B. Gold, M. Halpern, E. Komatsu, M. R. Nolta, L. Page, D. N. Spergel, E. Wollack, J. Dunkley, A. Kogut, M. Limon, S. S. Meyer, G. S. Tucker, and E. L. Wright. Nine-year Wilkinson Microwave Anisotropy Probe (WMAP) Observations: Final Maps and Results. *The Astrophysical Journal Supplement Series*, 208:20, October 2013.

[3] Planck Collaboration, N. Aghanim, M. Ashdown, J. Aumont, C. Baccigalupi, M. Ballardini, A. J. Banday, R. B. Barreiro, N. Bartolo, S. Basak, R. Battye, K. Benabed, J.-P. Bernard, M. Bersanelli, P. Bielewicz, J. J. Bock, A. Bonaldi, L. Bonavera, J. R. Bond, J. Borrill, F. R. Bouchet, F. Boulanger, M. Bucher, C. Burigana, R. C. Butler, E. Calabrese, J.-F. Cardoso, J. Carron, A. Challinor, H. C. Chiang, L. P. L. Colombo, C. Combet, B. Comis, A. Coulais, B. P. Crill, A. Curto, F. Cuttaia, R. J. Davis, P. de Bernardis, A. de Rosa, G. de Zotti, J. Delabrouille, J.-M. Delouis, E. Di Valentino, C. Dickinson, J. M. Diego, O. Doré, M. Douspis, A. Ducout, X. Dupac, G. Efstathiou, F. Elsner, T. A. Enßlin, H. K. Eriksen, E. Falgarone, Y. Fantaye, F. Finelli, F. Forastieri, M. Frailis, A. A. Fraisse, E. Franceschi, A. Frolov, S. Galeotta, S. Galli, K. Ganga, R. T. Génova-Santos, M. Gerbino, T. Ghosh, J. González-Nuevo, K. M. Górski, S. Gratton, A. Gruppuso, J. E. Gudmundsson, F. K. Hansen, G. Helou, S. Henrot-Versillé, D. Herranz, E. Hivon, Z. Huang, S. Ilic, A. H. Jaffe, W. C. Jones, E. Keihänen, R. Keskitalo, T. S. Kisner, L. Knox, N. Krachmalnicoff, M. Kunz, H. Kurki-Suonio, G. Lagache, J.-M. Lamarre, M. Langer, A. Lasenby, M. Lattanzi, C. R. Lawrence, M. Le Jeune, J. P. Leahy, F. Levrier, M. Liguori, P. B. Lilje, M. López-Caniego, Y.-Z. Ma, J. F. Macías-Pérez, G. Maggio, A. Mangilli, M. Maris, P. G. Martin, E. Martínez-González, S. Matarrese, N. Mauri, J. D. McEwen, P. R. Meinhold, A. Melchiorri, A. Mennella, M. Migliaccio, M.-A. Miville-Deschênes, D. Molinari, A. Moneti, L. Montier, G. Morgante, A. Moss, S. Mottet, P. Naselsky, P. Natoli, C. A. Oxborrow, L. Pagano, D. Paoletti, B. Partridge, G. Patanchon, L. Patrizii, O. Perdereau, L. Perotto, V. Pettorino, F. Piacentini, S. Plaszczynski, L. Polastri, G. Polenta, J.-L. Puget, J. P. Rachen, B. Racine, M. Reinecke, M. Remazeilles, A. Renzi, G. Rocha, M. Rossetti, G. Roudier, J. A. Rubiño-Martín, B. Ruiz-Granados, L. Salvati, M. Sandri, M. Savelainen, D. Scott, G. Sirri, R. Sunyaev, A.-S. Suur-Uski, J. A. Tauber, M. Tenti, L. Toffolatti, M. Tomasi, M. Tristram, T. Trombetti, J. Valiviita, F. Van Tent, L. Vibert, P. Vielva, F. Villa, N. Vittorio, B. D. Wandelt, R. Watson, I. K. Wehus, M. White, A. Zacchei, and A. Zonca. Planck intermediate results. XLVI. Reduction of large-scale systematic effects in HFI polarization maps and estimation of the reionization optical depth. *ArXiv e-prints*, May 2016.

[4] M. Hazumi, J. Borrill, Y. Chinone, M. A. Dobbs, H. Fuke, A. Ghribi, M. Hasegawa, K. Hattori, M. Hattori, W. L. Holzapfel, Y. Inoue, K. Ishidoshiro, H. Ishino, K. Karatsu, N. Katayama, I. Kawano, A. Kibayashi, Y. Kibe, N. Kimura, K. Koga, E. Komatsu, A. T. Lee, H. Matsuhara, T. Matsumura, S. Mima, K. Mitsuda, H. Morii, S. Murayama, M. Nagai, R. Nagata, S. Nakamura, K. Natsume, H. Nishino, A. Noda, T. Noguchi, I. Ohta, C. Otani, P. L. Richards, S. Sakai, N. Sato, Y. Sato, Y. Sekimoto, A. Shimizu, K. Shinozaki, H. Sugita, A. Suzuki, T. Suzuki, O. Tajima, S. Takada, Y. Takagi, Y. Takei, T. Tomaru, Y. Uzawa,

H. Watanabe, N. Yamasaki, M. Yoshida, T. Yoshida, and K. Yotsumoto. LiteBIRD: a small satellite for the study of B-mode polarization and inflation from cosmic background radiation detection. In *Space Telescopes and Instrumentation 2012: Optical, Infrared, and Millimeter Wave*, volume 8442, page 844219, September 2012.

[5] Christopher G. R. Wallis, Michael L. Brown, Richard A. Battye, and Jacques Delabrouille. Optimal scan strategies for future cmb satellite experiments. *Monthly Notices of the Royal Astronomical Society*, 466(1):425–442, 2017.

[6] P. Natoli, M. Ashdown, R. Banerji, J. Borrill, A. Buzzelli, G. de Gasperis, J. Delabrouille, E. Hivon, D. Molinari, G. Patanchon, L. Polastri, M. Tomasi, F. R. Bouchet, S. Henrot-Versillé, D. T. Hoang, R. Keskitalo, K. Kiiveri, T. Kisner, V. Lindholm, D. McCarthy, F. Piacentini, O. Perdereau, G. Polenta, M. Tristram, A. Achucarro, P. Ade, R. Allison, C. Baccigalupi, M. Ballardini, A. J. Banday, J. Bartlett, N. Bartolo, S. Basak, D. Baumann, M. Bersanelli, A. Bonaldi, M. Bonato, F. Boulanger, T. Brinckmann, M. Bucher, C. Burigana, Z. Y. Cai, M. Calvo, C. S. Carvalho, M. G. Castellano, A. Challinor, J. Chluba, S. Clesse, I. Colantoni, A. Coppolecchia, M. Crook, G. D'Alessandro, P. de Bernardis, G. De Zotti, E. Di Valentino, J. M. Diego, J. Errard, S. Feeney, R. Fernandez-Cobos, F. Finelli, F. Forastieri, S. Galli, R. Genova-Santos, M. Gerbino, J. González-Nuevo, S. Grandis, J. Greenslade, A. Gruppuso, S. Hagstotz, S. Hanany, W. Handley, C. Hernandez-Monteagudo, C. Hervías-Caimapo, M. Hills, E. Keihänen, T. Kitching, M. Kunz, H. Kurki-Suonio, L. Lamagna, A. Lasenby, M. Lattanzi, J. Lesgourgues, A. Lewis, M. Liguori, M. López-Caniego, G. Luzzi, B. Maffei, N. Mandolesi, E. Martinez-González, C. J. A. P. Martins, S. Masi, S. Matarrese, A. Melchiorri, J. B. Melin, M. Migliaccio, A. Monfardini, M. Negrello, A. Notari, L. Pagano, A. Paiella, D. Paoletti, M. Piat, G. Pisano, A. Pollo, V. Poulin, M. Quartin, M. Remazeilles, M. Roman, G. Rossi, J. A. Rubino- Martin, L. Salvati, G. Signorelli, A. Tartari, D. Tramonte, N. Trappe, T. Trombetti, C. Tucker, J. Valiviita, R. Van de Weijgaert, B. van Tent, V. Vennin, P. Vielva, N. Vittorio, C. Wallis, K. Young, and M. Zannoni. Exploring cosmic origins with CORE: Mitigation of systematic effects. *Journal of Cosmology and Astro-Particle Physics*, 2018:022, April 2018.

[7] Planck Collaboration, P. A. R. Ade, N. Aghanim, M. Arnaud, M. Ashdown, J. Aumont, C. Baccigalupi, A. J. Banday, R. B. Barreiro, J. G. Bartlett, and et al. Planck 2015 results. XII. Full focal plane simulations. *Astron. Astrophys.*, 594:A12, September 2016.

[8] Levon Pogosian and Alex Zucca. Searching for primordial magnetic fields with CMB B-modes. *Classical and Quantum Gravity*, 35(12):124004, May 2018.

[9] Planck 2018-VI. Planck 2018 results. VI. Cosmological parameters. July 2018.

[10] C. Rosset, M. Tristram, N. Ponthieu, P. Ade, J. Aumont, A. Catalano, L. Conversi, F. Couchot, B. P. Crill, F.-X. Désert, K. Ganga, M. Giard, Y. Giraud-Héraud, J. Haïssinski, S. Henrot-Versillé, W. Holmes, W. C. Jones, J.-M. Lamarre, A. Lange, C. Leroy, J. Macías-Pérez, B. Maffei, P. de Marcillac, M.-A. Miville-Deschênes, L. Montier, F. Noviello, F. Pajot, O. Perdereau, F. Piacentini, M. Piat, S. Plaszczynski, E. Pointecouteau, J.-L. Puget, I. Ristorcelli, G. Savini, R. Sudiwala, M. Veneziani, and D. Yvon. Planck pre-launch status: High Frequency Instrument polarization calibration. *A&A*, 520:A13+, September 2010.

[11] Planck collaboration. Planck intermediate results. XLIX. Parity-violation constraints from polarization data. *Astronomy and Astrophysics*, 596:A110, December 2016.

[12] Jonathan Aumont, Juan-Francisco Macias-Perez, Alessia Ritacco, Nicolas Ponthieu, and Anna Mangilli. Absolute calibration of the polarisation angle for future CMB B-mode experiments from current and future measurements of the Crab nebula. May 2018.